

Technology Mapping for Beyond-CMOS Circuitry with Unconventional Cost Functions

Dewmini Sudara Marakkalage*, Marcel Walter^{†‡}, Siang-Yun Lee*, Robert Wille^{†§}, Giovanni De Micheli*

* Integrated Systems Laboratory, EPFL, Lausanne, Switzerland

[†] Chair for Design Automation, Technical University of Munich, Germany

[‡] University of Bremen, Germany

[§] Software Competence Center Hagenberg GmbH, Austria

Abstract—With beyond-CMOS circuit technologies emerging from scientific endeavors in an effort to outperform transistor-based logic in feature size, operation speed, and energy dissipation, it has become apparent that besides their differences in physical implementations, their design automation techniques also have to evolve past established norms. While conventional logic synthesis aggressively optimizes the number of nodes in logic networks (as a proxy criterion for area, delay, and power improvements), this trope does not incorporate the additional costs caused by inverters and interconnects in the form of wire segments, signal splitters, and cross-over cells as imposed onto novel circuit implementations such as photonic crystals and field-coupled nanotechnologies. In this work, we propose a novel scalable technology mapping algorithm that captures these unconventional costs by utilizing subcircuit databases that are obtained by applying technology-aware exact physical design techniques. This overcomes the substantial quality loss that previously inevitably occurred when generating beyond-CMOS circuit layouts from conventionally optimized logic networks. Our method achieves average improvements of 84.5%, 74.5%, and 65.2% for the number of buffers, the number of crossings, and the critical path length, respectively, as compared to a state-of-the-art physical design algorithm for FCN circuits.

Index Terms—Logic Synthesis, Technology Mapping, Beyond-CMOS, Physical Design Constraints

I. INTRODUCTION

As Moore’s Law has lost momentum, alternative circuit technologies that transcend past conventional transistor-based logic are arising from studies into material science and physics. These beyond-CMOS devices promise enhancements over CMOS circuits in various aspects. While *Photonic Crystals* perform logic operations through wave interference of photons at the speed of light, for instance [1], [2], *Silicon Dangling Bonds* (SiDBs) conduct logic-in-memory computations via the repulsion of electric fields with ultra-low power dissipation [3]–[5]. Similar *Field-coupled Nanotechnologies* (FCN) [6] are, e.g., *Quantum-dot Cellular Automata* (QCA) [7], [8] and *Nanomagnet Logic* (NML) [9], [10].¹ While these and future emerging technologies have their own design constraints, some similarities that are not captured by conventional optimization criteria continue to reappear.

To this end, an abundance of design flows for emerging circuit technologies rely on conventional logic synthesis that aggressively optimizes the number of nodes in logic networks, e.g., represented as an *And-Inverter Graphs* (AIGs), before incorporating technology-specific constraints on the physical design level. When dedicated placement and routing tools attempt to legalize such sub-par logic networks, it

usually results in increased layout costs due to the prior negligence of, e.g., inverter and/or interconnect costs, which add to the total area, delay, and power metrics [11], [12] (see Section II-A).

In beyond-CMOS technologies, the interconnect costs come from a variety of constraints such as path-balancing, branching, and planarization (see Section II-A). In some such technologies, interconnect costs commonly dominate gate costs by several orders of magnitude [11]. Therefore, *optimizing logic networks primarily for their number of nodes can be counterproductive* as more important cost factors are completely ignored. For superconducting electronics technologies, there have been attempts to mitigate interconnect overheads due to path-balancing and branching constraints [13], [14]. However, in technologies such as FCN, the main source of interconnect cost is planarization; to the best of our knowledge, no prior work has considered such costs in logic synthesis.

In this work, we propose to avoid the substantial overhead incurred when generating beyond-CMOS circuit layouts from conventionally optimized logic networks by incorporating *recurring generic physical design constraints of emerging technologies* into the *logic synthesis step* through optimizing for *unconventional but realistic cost functions*. To this end, we present a technology mapping algorithm that utilizes databases of exact subcircuits implemented in specific technologies. Our proposed algorithm provides average improvements of 84.5%, 74.5%, and 65.2% for the number of buffers, the number of crossings, and the length of the critical path, respectively, compared to a state-of-the-art physical design algorithm for FCN. The proposed algorithm is not limited to a particular technology but applies to a wide range of non-conventional circuit implementations that may exhibit one or more of the generic design constraints discussed in Section II-A.

Organization of the paper: Section II describes background and related work. Section III presents our novel technology mapping approach. Section IV shows the experimental results and Section V concludes the paper with a brief discussion.

II. BACKGROUND

This section briefly discusses technology constraints of beyond-CMOS technologies, a general circuit model, and some related work on technology mapping.

A. Beyond-CMOS Technologies with Unconventional Costs

In conventional technology-independent logic synthesis, AIGs are often used as circuit representations. For NAND-based CMOS technologies, the AIG size (or depth) measured

¹New technologies are continually being proposed, but their physical details are not crucial for the motivation and comprehension of this work.

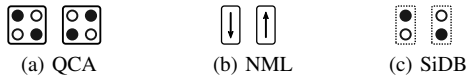


Fig. 1: Elementary FCN devices.

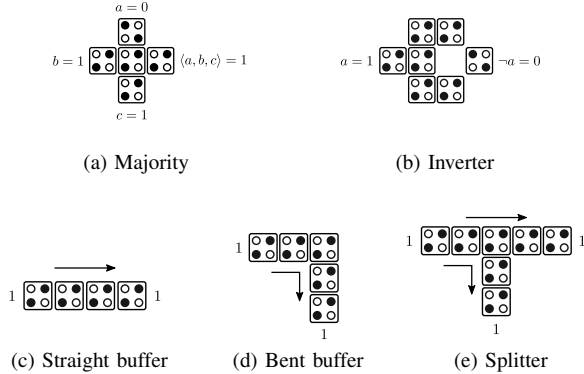


Fig. 2: QCA gates and wire segments.

in the number of AND gates in the network (or on the critical path) serves as a good estimation of the post-mapping area (or delay). However, in many emerging technologies, additional design constraints are imposed requiring special cells to be inserted to fulfill them; which increases the discrepancy between technology-independent and post-mapping layout cost metrics. There exists a plethora of beyond-CMOS technologies with such additional design constraints, and here we describe two such families. Due to this paper’s brevity, the technologies cannot be discussed in-depth. Instead, a general overview with a focus on cost functions is provided. We then identify a set of generic design constraints shared by many of these emerging technologies.

Field-coupled Nanocomputing (FCN): FCN is an umbrella term for a variety of nanotechnologies that have similar high-level models [6], and it contains *Quantum-dot Cellular Automata* (QCA) [7], [8], *Nanomagnet Logic* (NML) [9], [10], and *Silicon Dangling Bonds* (SiDBs) [3], [4]. Although their physical implementations differ, their concepts are nearly identical. In all cases, the information is represented by the polarization/magnetization of elementary nanometer-scale building blocks called *cells*. When placed in close proximity, cells influence each other’s polarization/magnetization through *Coulomb interaction*. Thus, they transmit information through electric/magnetic field coupling without a current flow [6], greatly reducing power dissipation and requiring less cooling than MOSFETs [12], [15]. Reversible FCN can operate below the *Landauer limit* [16], [17], a theoretical energy dissipation bound of non-reversible computation.

Fig. 1 shows elementary cells of aforementioned FCN technologies in the two binary states 0 (left) and 1 (right). The topological arrangements of cells form wire segments and gates that conduct Boolean operations, as shown in Fig. 2 for the QCA implementation [18]. During physical design, gates and wire segments are arranged in uniform *standard tiles* [19], [20], which can be viewed as building blocks that abstract physical effects to the logic design layer. Placement and routing of standard tiles attempt to create a layout from these building blocks that is functionally equivalent to a given logic network. Each tile has the same unit cost in both the

area and the delay regardless of whether it is a logic gate, a buffer, an inverter, or a splitter. FCN circuits are functionally sensitive to delays; signal paths of different lengths (in terms of the number of tiles) desynchronize, causing incorrect calculations [21].

Photonic Crystals: To realize complete optical logic circuits with information transmission at the speed of light, research has focused on photonic crystals, that is, optical nanostructures with periodically changing refractive indices [1]. This property allows or prohibits electromagnetic radiation to propagate through a photonic crystal based on its wavelength. Within the crystal lattice, *waveguides* [22] can be fabricated that restrict incoming light to propagating along certain channels; effectively creating wires for photons. At intersections, light originating from two different waveguides interferes to cancel out or amplify, based on its phase shift. This property has been used to envision optical Boolean gates [2]. However, interacting waveguides of different lengths can cause signals to desynchronize, thereby distorting or breaking gate functionality.

Unconventional design constraints and their costs: We consider the following unconventional costs that are shared by the aforementioned emerging technologies (and more) but not considered in conventional CMOS logic synthesis flows.

1. *Path-balancing buffers:* Due to the sensitivity to delay differences in signal paths, the path-balancing constraint is imposed, requiring that all paths from primary inputs to the fanins of the same gate have the same length. When shortening longer paths is not possible, buffer cells must be inserted into shorter paths to equalize the delay.

2. *Fanout-branching splitters:* Because the design of logic gates in these technologies does not naturally support driving multiple fanout signals, additional splitter cells need to be inserted at the output of multi-fanout gates to fulfill the fanout-branching constraint. Moreover, splitters are also counted in the path lengths of path balancing, thus, the fanout-branching and path-balancing constraints are strongly interwoven.

3. *Planarizing crossings:* The physical design of these technologies often requires special crossing cells to realize wire crossings in a 2-dimensional layout. The placement of logic gates may be altered to minimize such cases, but it is usually not possible to completely planarize the input network. Similarly to splitters, crossings also contribute to the path lengths and have to be considered together with path balancing. In some technologies, crossing cells are hard to fabricate or lead to less robust circuits due to their weaker signal strengths. In these cases, it is important to minimize the number of crossings, and unavoidable crossing cells lead to higher costs.

4. *Non-cost-free inverters:* Unlike traditional logic synthesis, where inverters (complemented edges) in AIGs do not contribute towards their size, inversion is not free in these technologies. It is not always possible to embed an inversion as a free negated input to a gate. Mitigating the effects of such inverters has been studied in [23]. However, these dedicated inverters not only increase the circuit size but also need to be considered together with the path-balancing constraint.

Through this consideration, it becomes apparent that cost metrics of conventional logic synthesis algorithms are not suited for the beyond-CMOS due to their negligence of the important aspects enumerated above.

B. Circuit Model

As we propose a new technology mapping algorithm supporting beyond-CMOS cost metrics, we locate this work at the intersection of logic synthesis (concerned with logic networks) and physical design (concerned with circuit layouts). The proposed algorithm’s output is a mixed logic network consisting of logic gates that are supported by a given technology library, which we represent as k -input look-up tables (k -LUTs), and special cells including path-balancing buffers, fanout-branching splitters, and planarizing crossings. To insert crossings in a meaningful way ensuring the network’s planarity, our mapping algorithm entails a coarse-grained placement with relative node positions. I.e., all cells in the mapped network are sorted into path-balanced ranks and are ordered within each rank.

Thereby, our algorithm outputs a partially placed, mapped network that 1) is functionally equivalent to the input network; 2) consists only of cells supported by the given technology library; and 3) satisfies all four constraints described in the previous section (path balancing, fanout branching, planarization, and dedicated inverters). Additionally, our algorithm aims to minimize the size and depth of this network model, which considers both logic gates and special cells. The area cost of each cell type can be parameterized to reflect the target technology as precisely as possible.

By considering such a circuit model, our size and depth evaluation is closer to the actual area and delay of the resulting layout after physical design. As design constraints are already satisfied and cells are ranked and ordered, the remaining placement and routing tasks become trivial for some technologies, but others may still need the network to be placed and routed according to the target layout topology, e. g., QCA layouts with non-linear clocking schemes [24], [25].

C. Conventional Technology Mapping

In typical logic synthesis flows, technology-aware optimizations are performed in the technology mapping stage, which happens after heavily optimizing a technology-independent representation with methods such as rewriting [26]. Technology mapping transforms a technology-independent logic representation into a technology-dependent one, where mapped circuits are obtained by substituting small sections with standard cells that represent the elements of the target technology. Numerous mapping algorithms have been proposed over the years [27], [28], but most such approaches are specific to CMOS-based synthesis flows and produce subpar results when used for emerging technologies as such methods were not targeting aforementioned unconventional costs.

III. PROPOSED METHODOLOGY

In this section, we describe the proposed novel technology mapping approach for beyond-CMOS technologies. While we use FCN as the exemplar technology because it has all four unconventional design constraints of Section II and it is a promising competitor in the beyond-CMOS domain due to recent fabrication breakthroughs [3], the proposed idea is generally applicable to other emerging technologies that require path-balancing, branching, and (optionally) planarization.

We propose generating 1) a design database of optimal subcircuits up to a certain number of inputs and 2) use it

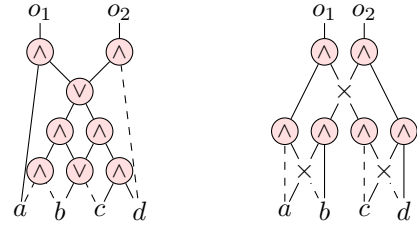


Fig. 3: Two realizations of a network computing $o_1 = a \wedge b \wedge c \wedge d$ and $o_2 = \neg a \wedge \neg b \wedge \neg c \wedge \neg d$. Inverters are denoted by dashed edges and crossing cells are denoted by a \times symbol.

during technology mapping to rewrite small logic blocks of larger networks. Although this idea has been considered before [26], it was only ever able to capture abstract technology-independent costs such as the size or depth of subcircuits. Instead, we generate the database with an optimal physical design algorithm tuned to the desired target technology, thus incorporating all elements of potential final circuit costs. Consequently, our technology mapper’s outputs inherently respect (configurable) inverter, buffer, splitter, and crossing costs,² thus they represent the final circuit layout much more closely and prevent overhead at the physical design stage.

To illustrate the need for technology-dependent optimizations in the logic synthesis stage, consider a circuit with input variables a, b, c, d that computes $o_1 = a \wedge b \wedge c \wedge d$ and $o_2 = \neg a \wedge \neg b \wedge \neg c \wedge \neg d$. Suppose that we are optimizing for a simplified technology with AND2 and OR2 gates, which has no inversion cost, but needs path-balancing and planarization with crossings. While there is a mapped configuration with 8 cells (Fig. 3 (left)), a naive technology-independent optimization might give a more compact representation with only 6 gates which need 9 cells in total including 3 additional crossing cells to meet the planarization constraint (Fig. 3 (right)).

A. Generation of Optimal Subcircuits

Conventional Boolean rewriting has successfully provided the groundwork for utilizing databases of optimal subcircuits. Usually, NPN canonization is utilized to significantly reduce the database sizes [26]. Two single-output Boolean functions belong to the same NPN class if one can be translated into the other by (optionally) negating (N) the primary inputs, permuting (P) the primary inputs, and negating (N) the primary output. The representative of each class is its lexicographically smallest member. Since inverters are considered to be cost-free in AIGs and input permutations can be neglected because no sense of fixed topology is employed, NPN canonization is a strong tool for complexity reduction and optimization.

However, in beyond-CMOS technologies, inverters matter, and input permutations can only be altered using costly crossings. Therefore, only considering NPN representatives is insufficient as the costs of members belonging to the same NPN class might substantially differ in the final layouts.

Therefore, we propose exploring a middle ground between the exhaustive enumeration of all 2^{2^n} Boolean functions in n variables and their NPN representatives. Namely, we rely on a class that we call NN that respects input/output permutations

²Although we focus on these four cost functions because they represent important roadblocks to overcome in contemporary emerging technologies, our general approach applies to arbitrary cost functions as long as there exists a physical design algorithm for generating the optimal design database.

Algorithm 1: Proposed technology mapping algorithm.

Input: Input network N and database DB.
Output: A technology-mapped version of N .

- 1 $N_{\text{lut}} \leftarrow N$ mapped to a 4-LUT network with ABC.
- 2 Assign levels to nodes in N_{lut} and fix the ordering of nodes.
- 3 $N_{\text{buf}} \leftarrow$ buffer inserted version of N_{lut} .
- 4 $N_{\text{xing}} \leftarrow$ crossing minimized version of N_{buf} .
- 5 $L \leftarrow$ number of logic levels in N_{xing} .
- 6 **foreach** level $\ell \in \{1, \dots, L\}$ **do**
- 7 $DesiredOrder \leftarrow []$.
- 8 **foreach** node n of level ℓ **do**
- 9 Reorder fanins of n to avoid self-crossings.
- 10 Update node function of n .
- 11 Append reordered fanins to $DesiredOrder$.
- 12 Construct buffer/splitter/crossing layers in N_{xing} to achieve the signal order of $DesiredOrder$ at the outputs of level $\ell - 1$.
- 13 **foreach** node n of level ℓ **do**
- 14 $(S, InvConfig) \leftarrow$ find best network structure and I/O inversion configuration for n from DB.
- 15 Replace n in N_{xing} with S after applying $InvConfig$.
- 16 Add buffers to N_{xing} to balance the outputs at level $\ell + 1$.
- 17 **return** N_{xing}

but not primary inversions. The number of NN classes is greater by a factor of $n!$ compared to NPN. For example, while the number of 4-input NPN classes is 222, our 4-input database has $222 \cdot 4! = 5328$ entries, which is still much smaller than the number of 4-input functions ($2^{2^4} = 65536$).

For each canonized (lexicographically smallest) NN representative, we generate an optimal (with respect to the imposed cost functions) subcircuit layout in the target technology. To this end, we modified an open-source physical design algorithm [29], [30] to compute the optimal FCN circuit layouts under different primary input permutations. Since that algorithm is based on SMT solving, we enforce the input permutation $\pi : x_1 \succ x_2 \succ \dots \succ x_n$ by adding an additional constraint. Let p_{xt} be the Boolean variable that, when set to 1, represents that node x is placed on layout tile t . To enforce that if a primary input is placed on some tile, any other primary input that follows in the permutation order must not be placed on a prior tile in the layout, the constraint is defined as: $\bigwedge_{t \in T, x \in \pi} (p_{xt} \implies \bigwedge_{t' \succ t, x' \succ x'} \neg p_{x't'})$. The inclined reader is referred to [29] for an in-depth explanation of existing constraints for valid node placement, wire routing, crossing insertion, path balancing, etc. Finally, incremental SMT solver calls that iteratively increase the available layout area for the physical design process ensure optimality of the eventually found result. Symmetry breaking allows effective search space pruning, and highly specialized cardinality constraint engines in the utilized Z3 solver [31] enable critical runtime reductions that keep the approach scalable up to ≈ 100 layout tiles, which is sufficient to realize all 4-input NN representatives.

B. Rewriting Using the Exact Database

This step decomposes the input network into small logic blocks and substitutes them using the appropriate optimum structures described in the previous section, while also synthesizing interconnections between logic blocks (Algorithm 1).

Decomposing into small logic blocks: Typical technology-mapping algorithms consider small cuts rooted at different nodes in the network and replace them with optimized versions, and when doing so, conventional algorithms give only minor importance to other fanouts of the cut leaves. However, to consider branching and planarization constraints

of emerging technologies, when replacing a cut, it is important to know the relative positions of the other fanouts of the cut leaves concerning the part that is being replaced to preserve already instantiated (partial-)planarization. To this end, we 1) fix the decomposition into small logic blocks by mapping the network to 4-LUTs using `if -K 4` command of the logic synthesis tool ABC [32] (Line 1), and 2) fix the relative positions of those logic blocks by assigning ranks to LUTs and imposing an ordering of the LUTs in each rank (Line 2).

Initial path-balancing and crossing optimization: Before rewriting LUTs, the algorithm decides the locations of wires between non-consecutive LUT logic levels. For example, if there is a LUT a in level 1 which is a fanin of a LUT d in level 3 and if level 2 has two LUTs b and c in that order, for proper planarization, the algorithm decides whether the wire from a to d goes through the space left of b , between b and c , or right of c . The initial path-balancing thus inserts buffers to denote such path propagation locations for each wire that connects non-consecutive LUT layers (Line 3). During LUT rewriting, these buffers are extended to buffer chains to meet the path-balancing constraint.

To minimize crossings, the initial buffers are inserted in a locally optimal way, keeping a fixed ordering of LUTs. I.e. for a LUT a in level ℓ , if a buffer needs to be inserted in level $\ell + 1$, it is placed at the location that minimizes the number of level- ℓ -to-level- $\ell + 1$ connections that cross the path from the LUT to the buffer. After buffer insertion, crossing optimization is performed for each level (Line 4) by swapping adjacent node pairs in each level as long as it leads to fewer crossings.

Substituting LUTs from the database entries: In the final step, the path-balanced network is reconstructed in a level-by-level fashion (Lines 6-16). Reconstructing level $\ell + 1$ consists of three main steps: 1) for each LUT in $\ell + 1$, their fanins are reordered to avoid crossings between pairs of their fanins, and the node functions are altered accordingly (Lines 9-10); 2) zero or more layers, each consisting of buffers/splitters/crossings, are inserted between level ℓ and $\ell + 1$ to obtain the fanins of level $\ell + 1$ in the correct order (Line 12); and 3) the LUTs in level $\ell + 1$ are replaced with the respective optimal structures from the database (Lines 14-15). The database includes entries for all 4-input NN classes but does not include all input/output inverted versions to avoid pre-computing the entire domain of 4-input functions. Hence, the algorithm considers all possible input/output inversions for LUT node functions and finds a match in the database. Then, the LUT is replaced with the found entry, after applying appropriate input/output inversions.

Run-time and space complexity: The run-time and space complexity of our algorithm is dominated by the crossing insertion between two consecutive levels in Line 12. If the number of gates in layer ℓ is n_ℓ and $m_\ell = \max(n_\ell, n_{\ell-1})$, then the worst-case for this step would need $\mathcal{O}(m_\ell)$ -many new layers each consisting of $\mathcal{O}(m_\ell)$ crossings/buffers (consider the case where outputs of level $\ell - 1$ are connected to the inputs of level ℓ in the opposite order). Thus the total run-time and space needed for this step is $\mathcal{O}(\sum_{\ell=1}^L m_\ell^2)$, which is $\mathcal{O}(n^2)$ in the worst-case where n is the size of the network. As the database of optimum substructures is computed for constant-sized functions, each database entry has constant size, and with proper indexing, the lookup is

TABLE I: Results of the proposed technology mapping approach on the ISCAS [33] and EPFL [34] benchmark suites.

	Benchmark Circuit					State of the Art [35]				Proposed Approach								
	Name	PI	PO	Gates	Depth	Total Nodes	Buffers	Crossings	CP	Total Nodes	Buffers	Crossings	CP	Runtime in sec.	Buffers impr. %	Crossings impr. %	CP impr. %	
ISCAS85 [33]	c17	5	2	6	3	99	69	16	26	63	31	6	13	0.04	55.1	62.5	50.0	
	c432	36	7	208	26	35 776	31 131	4201	701	14 910	12 170	1 973	299	0.06	60.9	53.0	57.3	
	c499	41	32	398	19	94 621	88 261	5456	1402	11 842	8754	1 948	227	0.06	90.1	64.3	83.8	
	c880	60	26	325	25	70 108	61 040	8438	1062	28 920	23 055	4 593	457	0.07	62.2	45.6	57.0	
	c1355	41	32	502	25	117 056	109 738	6198	1722	11 565	8521	1 936	219	0.06	92.2	68.8	87.3	
	c1908	33	25	341	27	77 950	71 177	5995	1201	17 201	14 026	2 187	364	0.06	80.3	63.5	69.7	
	c2670	157	64	716	20	323 824	281 067	41 267	2464	88 295	72 777	13 613	774	0.11	74.1	67.0	68.6	
	c3540	50	22	1024	41	587 468	531 807	53 498	3280	97 627	65 925	28 312	977	0.11	87.6	47.1	70.2	
	c5315	178	123	1776	37	1 864 282	1 710 369	150 222	5869	301 880	246 660	50 522	1504	0.27	85.6	66.4	74.4	
	c6288	32	32	2337	120	988 542	939 626	42 447	8901	97 313	73 052	15 542	1280	0.15	92.2	63.4	85.6	
	c7552	207	108	1469	26	1 481 318	1 351 266	126 753	5169	411 383	333 298	73 019	1797	0.36	75.3	42.4	65.2	
	EPFL [34]	adder	256	129	1020	255	794 313	708 447	83 316	4083	2 181 853	2 146 359	31 625	9350	1.65	-203.0	62.0	-129.0
		arbiter	256	129	11 839	87	61 392 432	56 342 578	5 025 982	36 160	7 432 960	6 661 959	731 089	11 646	6.10	88.2	85.5	67.8
		bar	135	128	3336	12	4 050 823	3 680 537	363 230	10 782	1 023 446	448 804	562 234	2369	0.63	87.8	-54.8	78.0
cavlc		10	11	693	16	286 509	259 800	25 100	2333	86 999	54 839	29 403	760	0.09	78.9	-17.1	67.4	
ctrl		7	26	174	10	28 188	25 097	2667	654	4480	2689	1 273	128	0.05	89.3	52.3	80.4	
dec		8	256	304	3	161 857	154 666	6871	1143	25 321	3859	19 894	215	0.06	97.5	-189.5	81.2	
i2c		147	142	1342	20	1 129 553	1 030 768	95 968	4568	294 762	238 114	52 198	1163	0.30	76.9	45.6	74.5	
int2float		11	7	260	16	48 219	42 793	4875	833	12 161	8175	3124	293	0.06	80.9	35.9	64.8	
max		512	130	2865	287	5 378 865	4 720 729	651 642	10 130	6 182 860	5 879 043	294 321	11 589	8.53	-24.5	54.8	-14.4	
priority		128	8	978	250	668 097	607 825	57 916	3477	290 810	273 901	13 407	2487	0.25	54.9	76.9	28.5	
router		60	30	257	54	54 074	45 627	7955	814	20 033	18 439	648	348	0.06	59.6	91.9	57.2	
sin		24	25	5416	225	8 237 614	7 711 879	514 234	16 990	1 145 537	934 129	192 740	6340	0.64	87.9	62.5	62.7	
voter		1001	1	13 758	70	53 955 839	50 500 625	3 421 110	48 864	3 375 273	2 734 141	601 139	5442	7.60	94.6	82.4	88.9	
div		128	128	57 247	4372			<i>out of memory</i>			104 918 980	101 310 752	3 409 196	249 354	56.49	—	—	—
hyp	256	128	214 335	24 801			<i>out of memory</i>			1 128 917 685	1 029 593 313	98 519 782	1 226 868	1172.27	—	—	—	
log2	32	32	32 060	444			<i>out of memory</i>			24 816 049	20 493 947	4 215 965	47 005	10.22	—	—	—	
mem_ctrl	1204	1231	46 836	114			<i>out of memory</i>			371 071 747	341 555 500	29 369 279	108 019	577.26	—	—	—	
multiplier	128	128	27 062	274			<i>out of memory</i>			33 370 845	28 610 811	4 668 200	28 842	16.83	—	—	—	
sqrt	128	64	24 618	5058			<i>out of memory</i>			41 768 215	41 226 185	470 491	169 800	26.22	—	—	—	
square	64	128	18 484	250			<i>out of memory</i>			17 588 918	14 252 309	3 266 047	14 747	7.36	—	—	—	
<i>Weighted average</i>														84.5	74.5	65.2		

also constant time; hence replacing the LUTs with optimum structures increases the run-time by only a constant factor.

IV. EXPERIMENTAL EVALUATION

This section constitutes a quantitative evaluation of the proposed technology mapping algorithm.

A. Experimental Setup

The proposed algorithm was implemented in C++ on top of the open-source tools *mockturtle* [36] and *fiction* [30] and evaluated using the *ISCAS85* benchmarks [33] and *EPFL Benchmark Suite* [34]. We generated a database of optimal FCN layouts—relying on state-of-the-art technology constraints [37]—implementing all 5328 canonical NN representatives as Verilog modules. (Total uncompressed size is 12MB.) We then applied the proposed technology mapping algorithm to all circuits in the aforementioned benchmark suites. We measured the resulting gate-level costs concerning the number of buffers (including splitters), number of crossings, and critical path (CP) length, and compared them with the results of the best available (to best of our knowledge) large-scale FCN physical design algorithm that can handle layouts with more than 100 million tiles [35]. The implementation of [35] is publicly available [30], which enabled us to run all experiments with the same set of configurations. All evaluations were run on a MacBook Pro M1 with 10 CPU cores, 16 GPU cores, and 32 GB of RAM.

B. Results

To enable a fair comparison, we applied both our proposed algorithm and the state-of-the-art FCN algorithm [35] to all benchmarks, without performing any prior logic optimization.

The obtained results are shown in Table I. It lists the initial properties of the benchmarks under *Benchmark Circuit*; the columns under *State of the Art* indicate the statistics of the FCN layouts generated by [35]; and those under *Proposed*

Approach show results obtained from our technology mapping algorithm when applied to the FCN domain. For both algorithms, it lists the number of total nodes, the number of buffers (including splitters) and crossings, and the critical path (CP) length. The last three columns show relative improvements in buffer, crossing, and CP costs. The final row states a weighted average for the reductions in costs across all benchmarks (excluding those for which the state of the art could not generate a solution).

The proposed method consistently achieves over 50% improvement in the CP length for all benchmarks except for three. A similar level of improvement is also evident in the numbers of crossings and buffers for most of the benchmarks within a similar run-time. The average reductions for the number of buffers, number of crossings, and CP length are 84.5%, 74.5%, and 65.2%, respectively, which is a major improvement over the state of the art. Moreover, our method is more scalable as it yields results for the seven EPFL benchmarks on which the state of the art ran out of memory.

On the downside, a degradation of the CP length for benchmark ‘adder’, and a similar order of magnitude degradation of the number of crossings for benchmark ‘dec’ can be noticed, which appear to be outliers. However, it is to be noted that the benchmark ‘adder’ exhibits an improvement in the number of crossings, and the benchmark ‘dec’ shows an improvement in the CP length. Generally, an increase in the number of crossings results in an increase in the CP length, but, as the results for these outliers suggest, this is not always the case. The CP length is more related to the maximum number of crossings a single wire has than to the total number of crossings. That is, if there is a single wire that crosses m other wires and no other pairs of wires cross, the planarization needs at least m crossing layers and thus increases the CP delay by m levels. On the other hand, even if there are m crossings between two layers, if each wire only crosses a handful of other wires, that structure can be planarized with much fewer crossing layers, so the CP length

will be small. Thus, to minimize the CP length, a better objective is to minimize the maximum number of crossings for any wire, rather than minimizing the total number of crossings.

Additionally, when our crossing optimization and planarization steps are applied directly to the ‘adder’ AIG without any LUT-mapping, it yields a much better CP length. This implies that LUT mapping results in an increased amount of crossings among the resulting LUT nodes, which, in turn, increases the number of logic levels due to crossings that occur in series. I.e., LUT mapping on ‘adder’ seems to over-optimize for LUT depth, inadvertently making it harder to planarize, because the LUT mapping stage is unaware of the technology constraints. Thus, it seems promising to conduct further research on technology-aware decomposition techniques, which will help mitigate such outlier situations.

V. CONCLUSION

Many technological implementations in the beyond-CMOS domain come with unconventional cost functions that are not respected by classical logic synthesis and, hence, cause significant overhead in the physical design stage.

In this paper, we proposed an algorithm for technology mapping of beyond-CMOS circuitry that respects these unconventional cost functions via the application of a physical design database of optimal circuit layouts that is employed for logic rewriting, thus capturing cost factors that would otherwise remain transparent to the logic synthesis. Via an experimental evaluation, we showed that the proposed algorithm delivers average improvements of 84.5%, 74.5%, and 65.2% for the number of buffers, the number of crossings, and the critical path length, respectively, as compared to a state-of-the-art physical design algorithm for FCN circuits. Furthermore, results could be obtained for the seven largest EPFL benchmark circuits on which the state of the art ran out of memory, proving our approach to be more scalable. Thereby, this work constitutes a major improvement for the design automation of several emerging beyond-CMOS technology classes, which enables the cost-effective realization and integration of large-scale circuits in this domain.

VI. ACKNOWLEDGEMENT

This work was supported by the SNF grant “Supercool: Design methods and tools for superconducting electronics” under Grant 200021_1920981.

REFERENCES

- [1] J. D. Joannopoulos, P. R. Villeneuve, and S. Fan, “Photonic crystals,” *Solid State Communications*, vol. 102, no. 2-3, pp. 165–173, 1997.
- [2] Y. Zhang, Y. Zhang, and B. Li, “Optical switches and logic gates based on self-collimated beams in two-dimensional photonic crystals,” *Optics Express*, vol. 15, no. 15, pp. 9287–9292, 2007.
- [3] T. Huff, H. Labidi, M. Rashidi, L. Livadaru, T. Diemel, R. Achal, W. Vine, J. Pitters, and R. A. Wolkow, “Binary Atomic Silicon Logic,” *Nature Electronics*, vol. 1, pp. 636–643, 2018.
- [4] R. A. Wolkow, L. Livadaru, J. Pitters, M. Taucer, P. Piva, M. Salomons, M. Cloutier, and B. V. C. Martins, *Silicon Atomic Quantum Dots Enable Beyond-CMOS Electronics*. Springer, 2014, pp. 33–58.
- [5] J. Pitters *et al.*, “Atomically Precise Manufacturing of Silicon Electronics,” *ACS Nano*, 2024.
- [6] N. G. Anderson and S. Bhanja, Eds., *Field-Coupled Nanocomputing - Paradigms, Progress, and Perspectives*, ser. Lecture Notes in Computer Science. Springer, 2014, vol. 8280.
- [7] C. S. Lent, P. D. Tougaw, W. Porod, and G. H. Bernstein, “Quantum Cellular Automata,” *Nanotechnology*, vol. 4, no. 1, p. 49, 1993.
- [8] C. S. Lent, B. Isaksen, and M. Lieberman, “Molecular quantum-dot cellular automata,” *Journal of the American Chemical Society*, vol. 125, no. 4, pp. 1056–1063, 2003.
- [9] R. P. Cowburn and M. E. Welland, “Room Temperature Magnetic Quantum Cellular Automata,” *Science*, vol. 287, no. 5457, 2000.
- [10] G. H. Bernstein, A. Imre, V. Metlushko, A. Orlov, L. Zhou, L. Ji, G. Csaba, and W. Porod, “Magnetic QCA systems,” *Microelectronics Journal*, vol. 36, no. 7, pp. 619–624, 2005.
- [11] F. Sill Torres, P. A. Silva, G. Fontes, M. Walter, J. A. M. Nacif, R. Santos Ferreira, O. P. Vilela Neto, J. F. Chaves, R. Wille, P. Niemann, D. Große, and R. Drechsler, “On the Impact of the Synchronization Constraint and Interconnections in Quantum-dot Cellular Automata,” *Microprocessors and Microsystems*, vol. 76, pp. 103–109, 2020.
- [12] J. Timler and C. S. Lent, “Power Gain and Dissipation in Quantum-dot Cellular Automata,” *Journal of Applied Physics*, vol. 91, no. 2, 2002.
- [13] S.-Y. Lee, H. Rienner, and G. De Micheli, “Beyond local optimality of buffer and splitter insertion for aqf circuits,” in *Proceedings of the 59th ACM/IEEE Design Automation Conference*, 2022, pp. 445–450.
- [14] G. Pasandi and M. Pedram, “Pbmap: A path balancing technology mapping algorithm for single flux quantum logic circuits,” *IEEE Transactions on Applied Superconductivity*, vol. 29, no. 4, pp. 1–14, 2018.
- [15] E. Blair and C. Lent, “Clock Topologies for Molecular Quantum-Dot Cellular Automata,” *Journal of Low Power Electronics and Applications*, vol. 8, no. 3, 2018.
- [16] R. W. Keyes and R. Landauer, “Minimal Energy Dissipation in Logic,” *IBM Journal of Research and Development*, vol. 14, no. 2, 1970.
- [17] R. Landauer, “Irreversibility and Heat Generation in the Computing Process,” *IBM Journal of Research and Development*, vol. 5, 1961.
- [18] C. S. Lent and P. D. Tougaw, “A device architecture for computing with quantum dots,” *Proceedings of the IEEE*, vol. 85, no. 4, April 1997.
- [19] J. Huang, M. Momenzadeh, L. Schiano, M. Ottavi, and F. Lombardi, “Tile-based QCA Design Using Majority-like Logic Primitives,” *JETC*, vol. 1, no. 3, pp. 163–185, 2005.
- [20] D. A. Reis, C. A. T. Campos, T. R. B. S. Soares, O. P. V. Neto, and F. S. Torres, “A methodology for standard cell design for QCA,” in *ISCAS*, 2016, pp. 2114–2117.
- [21] F. S. Torres, M. Walter, R. Wille, D. Große, and R. Drechsler, “Synchronization of Clocked Field-Coupled Circuits,” in *IEEE-NANO*, 2018.
- [22] S. G. Johnson, P. R. Villeneuve, S. Fan, and J. D. Joannopoulos, “Linear waveguides in photonic-crystal slabs,” *Physical Review B*, vol. 62, 2000.
- [23] E. Testa, M. Soeken, O. Zografos, L. Amaru, P. Raghavan, R. Lauwereins, P.-E. Gaillardon, and G. De Micheli, “Inversion optimization in majority-inverter graphs,” in *NANOARCH*. Ieee, 2016, pp. 15–20.
- [24] C. A. T. Campos, A. L. Marciano, O. P. V. Neto, and F. S. Torres, “USE: A Universal, Scalable, and Efficient Clocking Scheme for QCA,” *IEEE Trans. Comput. Aided Des. Integr. Circuits Syst.*, vol. 35, no. 3, 2015.
- [25] M. Goswami, A. Mondal, M. H. Mahalat, B. Sen, and B. K. Sikdar, “An Efficient Clocking Scheme for Quantum-dot Cellular Automata,” *International Journal of Electronics Letters*, vol. 8, no. 1, 2020.
- [26] A. Mishchenko, S. Chatterjee, and R. K. Brayton, “DAG-aware AIG rewriting: A fresh look at combinational logic synthesis,” in *DAC*, E. Sentovich, Ed., 2006, pp. 532–535.
- [27] J. Cong and Y. Ding, “Flowmap: An optimal technology mapping algorithm for delay optimization in lookup-table based FPGA designs,” *IEEE Trans. Comput. Aided Des. Integr. Circuits Syst.*, vol. 13, 1994.
- [28] Y. Kukimoto, R. K. Brayton, and P. Sawkar, “Delay-optimal technology mapping by DAG covering,” in *DAC*, 1998, pp. 348–351.
- [29] M. Walter, R. Wille, D. Große, F. S. Torres, and R. Drechsler, “An exact method for design exploration of quantum-dot cellular automata,” in *DATE*, 2018, pp. 503–508.
- [30] M. Walter, R. Wille, F. S. Torres, D. Große, and R. Drechsler, “fiction: An open source framework for the design of field-coupled nanocomputing circuits,” 2019.
- [31] L. d. Moura and N. Bjørner, “Z3: An efficient SMT solver,” in *International Conference on Tools and Algorithms for the Construction and Analysis of Systems*, 2008, pp. 337–340.
- [32] R. Brayton and A. Mishchenko, “ABC: An academic industrial-strength verification tool,” in *CAV*, 2010, pp. 24–40.
- [33] F. Brgles and H. Fujiwara, “A neutral netlist of 10 combinational circuits and a target translator in fortran,” in *ISCAS*, 1985.
- [34] L. Amaru, P.-E. Gaillardon, and G. De Micheli, “The EPFL combinational benchmark suite,” in *IWLS*, 2015.
- [35] M. Walter, R. Wille, F. S. Torres, D. Große, and R. Drechsler, “Scalable design for field-coupled nanocomputing circuits,” in *ASP-DAC*, 2019.
- [36] M. Soeken, H. Rienner, W. Haaswijk, E. Testa, B. Schmitt, G. Meuli, F. Mozafari, S.-Y. Lee, A. Tempia Calvino, D. S. Marakkalage, and G. De Micheli, “The EPFL logic synthesis libraries,” 2022.
- [37] M. Walter, S. S. H. Ng, K. Walus, and R. Wille, “Hexagons are the bestagons: design automation for silicon dangling bond logic,” in *DAC*, 2022, pp. 739–744.